Available online at www.sciencedirect.com
SCIENCE DIRECT®
ACADEMIC PRESS
ICARUS
Icarus 162 (2003) 278–284
www.elsevier.com/locate/icarus

Speckle interferometry observations of asteroids at TNG☆

A. Cellino,[a,*] E. Diolaiti,[b] R. Ragazzoni,[c] D. Hestroffer,[d] P. Tanga,[e] and A. Ghedina[f]

[a] *INAF - Osservatorio Astronomico di Torino, 10025 Pino Torinese (TO), Italy*
[b] *Department of Astronomy, University of Padova, 35122 Padova, Italy*
[c] *INAF - Osservatorio Astronomico di Arcetri, 50125 Firenze, Italy, and Max-Planck-Institut für Astronomie, 69117 Heidelberg, Germany*
[d] *IMCCE, UMR CNRS 8028, Observatoire de Paris, 75014 Paris, France*
[e] *INAF - Osservatorio Astronomico di Torino, 10025 Pino Torinese (TO), Italy, and Observatoire de la Cote d'Azur, Nice, France*
[f] *INAF - Telescopio Nazionale Galileo, 38700 Santa Cruz de La Palma, Tenerife. P.O. Box 565, Spain*

Received 24 May 2002; revised 14 November 2002

Abstract

The Speckle camera of the 3.5 m Telescopio Nazionale Galileo (TNG) has been used to measure apparent sizes and shapes of a number of main belt asteroids. The average size measurements are in a generally good agreement with the results of indirect IRAS-based radiometric techniques. The measured shapes are compared with predictions based on previously derived spin axis directions and lightcurve photometry of some of the observed objects. Also in this case the agreement is reasonable and the speckle observations allow us to discriminate in some cases between the two pole solutions usually found for each object. No clear evidence of binaries was found. The results show that the TNG speckle camera can be a powerful tool to resolve relatively large main belt asteroids and to calibrate the results of the IRAS survey.

Keywords: Asteroids

1. Introduction

The development of techniques of high-resolution imaging, and the steady improvement of telescopic performances, due also to the availability of increasingly larger instruments, is starting to produce a major breakthrough in modern asteroid science.

For a long time, asteroids observed by means of ground-based telescopes have been point-like sources in all practical respects, apart from a very limited number of larger objects, whose apparent angular sizes were measured by pioneering studies using state-of-the-art techniques. Speckle interferometry has been used for this purpose (Baier and Weigelt, 1983; Drummond et al., 1985a, 1985b, 1988; Drummond and Christou, 1994; Drummond and Hege, 1986; Tsvetkova et al., 1991) and has produced those that for a long time have been very rare cases of *direct* measurements of asteroid sizes, apart from a number of observations of star occultations. The problem of the latter technique is that several chords measured by observers located in different locations along the occultation track are needed to derive reliable sizes and shapes, and this is rarely achievable in practice. As a consequence, the number of direct, reliable size measurements of asteroids has been extremely limited so far. More recently, size determinations have been obtained by means of adaptive optics (Drummond et al., 1998), by HST observations (Storrs et al., 1999), and in a few cases by spacecraft *rendezvous* or fly-bys.

Nevertheless, it is still true that most of the available information about the sizes of asteroids has come so far from indirect techniques such as radiometry and polarimetry. Currently, the IRAS catalog (the most updated release having been recently published by Tedesco et al., 2002) contributes to the largest part of the available database on asteroid sizes and albedoes, with a quantitatively minor contribution coming also from polarimetry (see, *e.g.*, Cellino et al., 1999).

☆ Based on observations carried out at the Telescopio Nazionale Galileo, operated by the Italian C.N.A.A.

* Corresponding author. Fax: +39-0118101930.
E-mail address: cellino@to.astro.it (A. Cellino).

0019-1035/03/$ – see front matter
doi:10.1016/S0019-1035(03)00006-X

Table 1
Observing circumstances

Object	Observation (Date/TU)	R. A. (h m s)	Dec. (° ′ ″)	Phase Angle	V Mag.	Air Mass
3 Juno	29/09/2000 / 22:45:00	20 51 09.5	−11 30 07	19.6	9.3	1.40
12 Victoria	01/10/2000 / 03:30:00	02 40 20.5	+22 22 44	16.1	10.3	1.00
16 Psyche	01/10/2000 / 05:30:00	05 17 40.9	+19 14 49	21.6	10.5	1.01
30 Urania	01/10/2000 / 02:00:00	02 22 22.2	+18 03 34	14.5	10.3	1.04
88 Thisbe	30/09/2000 / 22:00:00	23 53 45.8	+08 53 36	4.3	10.2	1.29
135 Hertha	30/09/2000 / 23:30:00	21 30 38.0	−14 50 32	22.4	11.0	1.50
230 Athamantis	01/10/2000 / 00:50:00	02 20 41.3	+23 19 27	14.3	10.4	1.10
324 Bamberga	01/10/2000 / 04:45:00	03 19 29.5	+37 13 47	27.5	9.4	1.03
90 Antiope	30/09/2000 / 00:30:00	00 02 18.6	−03 15 32	3.0	12.1	1.18

On the other hand, the increasing resolving power of modern telescopes can now be exploited to perform direct measurements of asteroid sizes and shapes in a much larger number of cases than previously possible. There are at least three excellent reasons to dedicate a special effort to high-resolution imaging of asteroids.

1. The direct measurement of sizes is needed to calibrate the available radiometric dataset in order to better understand the actual size distribution of the asteroid population.

2. There is the possibility of finding binary systems, as shown by recent exciting results based on adaptive optics (Merline et al., 1999, 2000). In turn, binaries give a rare opportunity to infer the *masses* of the components. The number of known binary systems among asteroids is steadily growing also as a consequence of radar observations of near-Earth asteroids, which have led to the discovery of a number of systems, including both contact and detached binaries (Ostro et al., 2003).

3. Since the number of asteroids for which a mass estimate can be possible will increase in the near future (due to the discovery of binaries and to the astrometric measurements of mutual gravitational perturbations) it is becoming essential to derive reliable volume estimates in order to compute average densities. Moreover, densities can also be estimated on the basis of the observed shapes and spin rates, under the assumption that the objects have equilibrium shapes, as suggested by a number of observational data, mainly for the largest objects of the asteroid main belt Cellino et al., 1987, 1989; Farinella et al., 1981, 1982).

For the above reasons, we have started a dedicated campaign of observations using the speckle camera of the Telescopio Nazionale Galileo (TNG), located on the Roque de los Muchachos in the Canary Islands. Some preliminary tests were already performed in 1999 during the commissioning phase of the adaptive optics module of TNG by Ragazzoni et al. (2000), who observed the two large asteroids 10 Hygiea and 15 Eunomia.

The first successful run of the present campaign was carried out in September 2000. In this paper we present the results of these observations, which have produced a relevant sample of directly measured sizes and shapes of main belt asteroids. Some discussion and implications of these preliminary results are also discussed.

2. The Observations

Speckle interferometry is a well known technique to obtain images close to the theoretical diffraction limit of modern telescopes. In its most preliminary form, limited to the possibility of obtaining the auto-correlation functions of the images of celestial bodies, it was first proposed by Labeyrie (1970). This is also the technique we used in our observations. A detailed description of the TNG speckle facility is given by Marchetti et al. (1997). Basically, the instrument records the accumulated power spectrum of target objects (in this case asteroids) and nearby stars used as calibrators to derive the speckle transfer function (STF). This is the Fourier transform of the autocorrelation of the point spread function and depends on both the telescope aperture and the atmospheric conditions (see, *e.g.,* Christou, 1988). STF is the basic quantity to be determined to derive the undistorted power spectrum of the target objects, from which evidence of binarity or measurements of the angular sizes of resolved disks can be obtained.

The acquisition system at TNG is efficient and produces a large amount of data that can be reduced using almost automated techniques. The major limitation is that individual speckle frames taken during the night are not stored, making it impossible to recover any information on the phase of the Fourier spectra. The Fourier phase is what describes the deviations from the symmetry of reflection through the center of the image. In this way, for instance, one can find evidence of binarity, but it is not possible to say which component is brighter.

The observations were carried out during two nights, on September 29 and 30, 2000. Table 1 lists the circumstances of observation of our targets. The seeing was fairly good during the first night, staying generally around or slightly below 1 arcsec. The situation was worse during the second night, with seeing steadily deteriorating from 1 arcsec at the beginning up to more than 2 arcsec at the end of the night.

For this reason, we were forced to discard some data obtained for the asteroid 16 Psyche, due to the low quality of the resulting power spectra.

In principle, the observed power spectra are contaminated by two main bias sources: the additive contribution of the detector noise and the so-called photon bias associated to the power spectrum of the pixel response. The former was estimated by averaging the pixels in the corners of the observed frame, outside the cutoff frequency imposed by the optical system; the latter was estimated from the observations of a flat source, namely a void region of the sky. The detector and the photon bias were removed from the observed power spectra following the procedure outlined by Christou (1988).

After this preliminary calibration step, the power spectrum of each asteroid was divided by the corresponding STF in order to filter the seeing effect. The undistorted power spectrum was then approximated by means of an elliptical gaussian, characterized by three unknown parameters, namely the length of the two axes and an orientation angle. The model choice is justified by our simulations of objects with surface brightness following a Minnaert law (see below): we verified in fact that the power spectrum of such objects can be accurately modeled by a gaussian shape. Furthermore this choice is in agreement with a previous analysis performed by Ragazzoni et al. (2000). The optimization of the parameters for each power spectrum was performed by an iterative fitting technique, excluding from the fit the pixels affected by an excessive noise contamination. In some cases we experienced an instability problem, which forced us to adopt a slightly different strategy: we estimated first the position angle of the elliptical gaussian and then we determined the axes of the model with the usual fitting procedure, but keeping the previously determined position angle fixed. The measurement of the angle in these cases was performed by slicing the power spectrum along different axes and determing the one with the largest width, obviously associated to the orientation angle of the power spectrum itself. Figure 1 shows as an example of the different steps of the overall procedure some results referring to the observations of the asteroid 12 Victoria. The top panels show the rough accumulated power spectra of the asteroid (top left) and the STF (top right). The lower panels show the resulting calibrated power spectrum of the object (after dividing by the STF) and the resulting best-fit elliptic gaussian.

The axes of the best-fit gaussian are inversely proportional to the corresponding axes of an assumed elliptical shape of the object. A careful calibration is needed here in order to convert the width of the power spectrum in the Fourier space into the corresponding size of the object in the image space. To do this, we carried out a set of stimulations in which we modeled the light distribution across the resolved elliptical disk of an asteroid using a simple limb-darkening Minnaert law, according to the formula

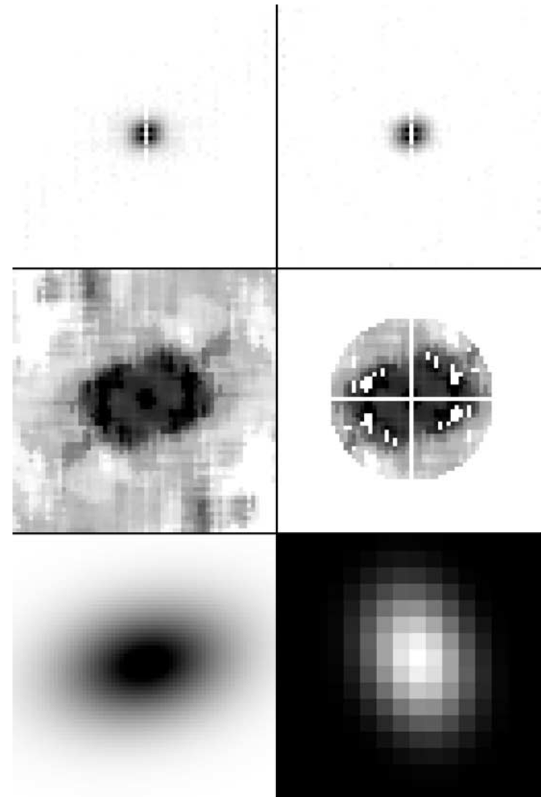

Fig. 1. As an example of some steps in the data reduction procedure, we show the recorded power spectrum of 12 Victoria, after removing the detector and photon bias (top left); the same but for the reference star (speckle transfer function) (top right); the resulting power spectrum of 12 Victoria after dividing by the STF (middle left); the same, but with the pixels not used in the fit procedure indicated (as blanks) (medium right); the best-fit elliptic gaussian corresponding to the derived power spectrum of Victoria (bottom left); and the corresponding reconstructed "image" of the object (bottom right).

$$I(\mu) = \mu^{2k-1},$$

where μ is the cosine of the angle between the normal to the surface and the line of sight to the observer. In principle, the above approximation of the limb-darkening effect holds for zero-phase angle, which is strictly not the case in our observations. In some cases we have observed objects at phase angles around or larger than 20 degrees. In these cases it is clear that the effect of the not fully illuminated disk can affect the determination of the axial ratios of the objects, although we did not make a direct quantitative estimate of this, since it would require a quite extensive work of numerical simulations (the effect depends on the shape itself, the spin axis direction, and the observational circumstances). For objects observed at lower phase angles, we do not expect that this effect can significantly influence our results, but in any case it is clear that the actual uncertainties in our determinations of the axial rations are larger than the nominal errors of the axial ratio solutions corresponding to the data reduction procedure explained in what follows. In practice, a set of Minnaert models was simulated, charac-

Table 2
Measured lengths of the axes *a, b* of the ellipses fitting the resolved disks of the observed asteroids, and corresponding position angles ϕ of these ellipses in the plane of sky (measured with respect to the north direction, the east corresponding to $\phi = 90°$)

Object	*a* (arcsec)	*b* (arcsec)	Φ (°)	*a* (km)	*b* (km)	$< D >$ (km)	*b/a*
3 Juno	0.23 ± 0.04	0.23 ± 0.04	—	287	287	287	1
12 Victoria	0.17 ± 0.03	0.12 ± 0.02	39 ± 1	158	112	133	0.71
16 Psyche	0.21 ± 0.04	0.17 ± 0.03	34 ± 1	315	262	288	0.83
30 Urania	0.13 ± 0.02	0.11 ± 0.02	84 ± 5	111	89	99	0.80
88 Thisbe	0.18 ± 0.03	0.15 ± 0.03	48 ± 5	191	163	176	0.85
135 Hertha	0.11 ± 0.02	0.09 ± 0.01	50 ± 1	93	74	83	0.80
230 Athamantis	0.15 ± 0.02	0.12 ± 0.02	85 ± 1	147	112	128	0.76
324 Bamberga	0.28 ± 0.05	0.28 ± 0.05	—	205	205	205	1

Note. The axis lengths are given in both arcsec and corresponding km (the latter corresponding to the nominal value measured in arcsec). The average size $< D >$ is computed as $\sqrt{a \cdot b}$. The axial ratios *b/a* are also given.

terized by a different limb-darkening coefficient k in a reasonable range ($0.5 \leq k \leq 0.7$), in agreement with the analysis performed by Ragazzoni et al. (2000). We note also that a value $k = 0.60$ is suggested by the analyses by Hestroffer (1998) and Parker et al. (2002), while Hestroffer and Mignard (1997) found $k = 0.65$ in the case of asteroid 1 Ceres. The fitting procedure described above, based on the gaussian model, was applied to the power spectrum of each synthetic object, retrieving the proportionality constant to convert the inverse width of the power spectrum to the known angular size of the object. Finally, the average of all the derived calibration constants was applied as a unique calibration constant for all the observed objects. Clearly this method introduces some errors, due to the fact that an average calibration constant was adopted and that the surface brightness of the observed object is actually unknown. We estimate however that the error in the sizes due to these uncertainties should not exceed ±5%.

The last step of the data reduction procedure was the correction of the estimated angular sizes and position angles, to account for the orientation of the speckle camera and for the geometric distortion of the detector, which were determined by means of observations of binary stars, comparing the retrieved parameters (separation and position angle) with the literature data. In particular the orientation of the camera introduces an offset in the position angle of the object, which is corrected very easily; more subtle is the effect of the distortion, which affects the estimated elliptical shape, modifying both the length of the axes and the position angle.

The final results (axes a and b in arcsec and position angles Φ) are listed in Table 2 for each object, together with the corresponding absolute sizes in km (nominal values) and resulting average diameter (defined here as the square root of the *ab* product). The axial ratio *b/a* is also listed in each case. Due to all the possible sources of uncertainty mentioned above, including also the role of non-negligible phase angles at the epochs of observation, we do not expect the real uncertainties in the sizes and axial ratios to be much better than 10–15%.

In a couple of cases, the obtained power spectra turned out to be so slightly elongated that a circular solution must be accepted. Of course, in such cases the Φ angle loses any meaning.

We note also that the observations are inherently short and thus produce a kind of instantaneous picture of the apparent size and shape of each object, not significantly blurred by the effect of spin around the rotation axis.

3. Comparison with IMPS and photometric data

All the objects observed in this campaign have published values of size. The most important dataset of asteroid sizes and albedoes to which we refer here is the *Supplemental Infrared Minor Planet Survey* (SIMPS), obtained from the radiometric observations performed by the IRAS satellite (Tedesco et al., 2002).

A knowledge of the average sizes of the objects is essential for physical studies of asteroids. Moreover, the overall size distribution of the population that we observe today is thought to be the result of a long process of collisional evolution that has been active since the early epochs of Solar System history. The current size distribution is an essential constraint for any model aimed at reproducing the collisional history of the belt and determining the properties of the primordial population of objects at the beginning of the collisional regime (Campo Bagatin et al., 1994). It is also critically needed to evaluate the current inventory of the asteroid population down to small sizes, which are very important for estimating the likely flux of bodies from the main belt into the region of the terrestrial planets (see, *e.g.*, Zappalà and Cellino, 2001). For the above reasons, the possibility to obtain a direct measurement of asteroid sizes is important to confirm the overall reliability of the IRAS dataset, which is based on an indirect technique of size and albedo determination (see, *e.g.*, Tedesco, 1994).

It is also important that for some of the objects that we have observed, estimates of the coordinates of the spin axis are available as well as an associated estimate of the axial ratios *b/a* and *c/a* (assuming for the objects triaxial ellipsoid shapes with axes $a > b > c$). These pole and shape estimates come from analyses of published lightcurves obtained at different apparitions and aspect angles. In general (Magnusson et al., 1989) photometry does not allow the observers to derive a unique solution for the pole coordinates. Instead, an ambiguity is normally present, with a couple of distinct pole solutions both being compatible with the photometric data. Moreover, in some cases, the adopted techniques of pole determination do not give an indication of the sense of spin of the object, but they only give the orientation of the spin axis in the celestial sphere. In principle, a direct observation of the elongation and orientation of the elliptical projection of the object on the sky at a given epoch can solve the pole ambiguity and, when present, can also solve the ambiguity on the sense of spin of the object.

In Table 3 we have listed for each object observed in our campaign the nominal SIMPS diameter and, when available, some nominal pole solutions published in the literature (available at the PDS database, at http://pdssbn.astro.umd.edu/sbnhtml/index.html). Associated with each pole and shape solution, there is a computation of the predicted axial ratio and orientation of the corresponding apparent ellipse of the object as observed in the sky at the epochs of our observations. As an example, we show in Fig. 2 the predicted appearance of asteroid 12 Victoria (based on the pole solution $\lambda = 9°$, $\beta = +55°$, and the corresponding axial ratio solution $a{:}b{:}c = 1.25{:}1{:}1$) at the epoch of our observations.

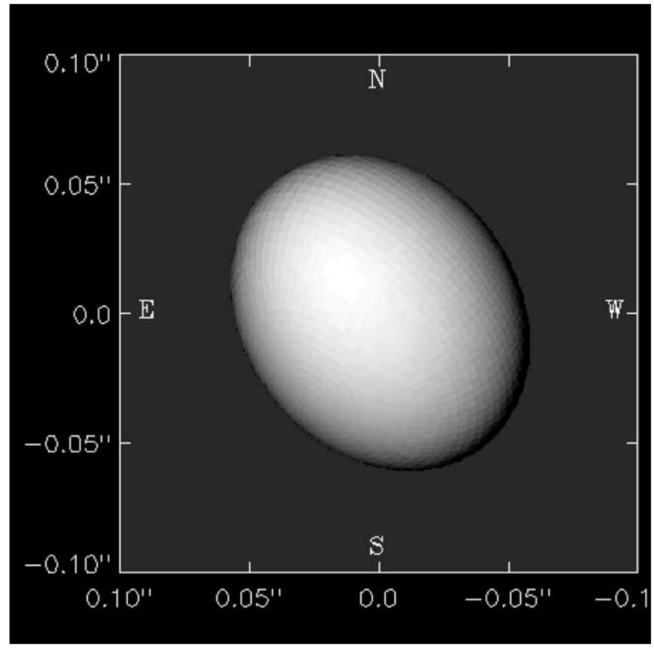

Fig. 2. Predicted appearance in the plane-of-sky view of the asteroid 12 Victoria at the epoch of our speckle observations (Fig. 1). This is given on the basis of the published pole solution ($\lambda = 9°$, $\beta = +55°$) and an ellipsoid solution $a \times b \times c = 65 \times 52 \times 52$ km.

Table 3
IRAS diameter and expected axial ratios and orientations according to the different pole coordinates published (when available) for each object observed in the present campaign.

Object	D_{IRAS} (km)	Pole Ecliptic coordinates B1950		*b/a*	Φ (°)
		λ(°)	β(°)		
3 Juno	233.9	108	+36	0.80	119
		318	+60	0.78	64
12 Victoria	112.8	9	+55	0.81	37
		189	−55	0.89	0
		176	+40	0.85	129
		356	−40	0.94	179
16 Psyche	253.2	35	−21	0.68	147
		215	−15	0.68	24
30 Urania	100.2	—	—	—	—
88 Thisbe	200.6	40	+70	0.86	71
		200	+70	0.82	63
135 Hertha	79.2	106	+02	0.82	58
		286	−02	0.81	82
		118	+52	0.86	49
		298	−52	0.77	61
		291	+47	0.86	91
		111	−47	0.78	77
230 Athamantis	109.0	—	—	—	—
324 Bamberga	229.4	—	—	—	—

Note. Pole solutions for which $\lambda_1 = \lambda_2 + 180$ and $\beta_1 = -\beta_2$ correspond to the same spin axis direction, but with the two alternative possibilities for the sense of rotation.

It should be noted that the computation of the rotational phase at the epochs of observation is based on an analysis of the most recently observed lightcurves and on the knowledge of the sidereal period of the objects. Some uncertainties are certainly present, since the determination of the precise instant of a particular lightcurve feature (generally the maximum) to be used as a reference to compute the rotational phase at the epoch of our observations is subject to non-negligible errors. The effect can be significant on the resulting axial ratio and orientation of the computed apparent ellipse. We should note also that the possible pole solutions listed for each object do not produce necessarily very large differences in the resulting axial ratio and position angle at the epochs of our observations. Moreover, our speckle-based determinations of the position angles are often significantly uncertain, at least in cases in which the resulting ellipse turned out to be only slightly elongated.

It is also clear that our data alone cannot be used to derive an estimate of the overall triaxial shapes of the objects, but only the sizes of the apparent ellipses projected on the sky at the epochs of observation. As a consequence, our average diameters are only an approximation of the real average size of the objects. This is true for whatever observation technique applied only at a single epoch of observation. More accurate measurements of the average sizes and overall shapes can be obtained only by means of additional observations taken at different rotation and aspect angles. Even taking into account the above caveats, some conclusions can be derived from our data. First of all, the average diameters turn out to be in generally good agreement with the IRAS-based results. The average discrepancy between our size determinations and those listed in the SIMPS catalog for the same objects of our sample is less than 15%. A systematic difference of less than +7% (the speckle-derived sizes being on the average larger than the radiometric ones) is found. The IRAS observations were generally obtained at different values of aspect and rotational phase; then the resulting discrepancies with our measurements, taking also into account the intrinsic errors of the two techniques, are fully reasonable and within the limits one could expect a priori in the case that the real shapes are not too exotic. This seems an important confirmation of the overall reliability of radiometric sizes and albedoes using the standard thermal model for main belt asteroids in this range of sizes (Tedesco, 1994).

The only really large discrepancy between our speckle-derived sizes and the published IRAS diameters concerns 3 Juno, and it is not clear to us if this was due to some possible instrumental problem. An intrinsic difficulty with 3 Juno is due to its large apparent angular size, because this means that the corresponding width of the recorded power spectrum was significantly small. This made it difficult to obtain a good fit, and in particular we found no convincing evidence of an elliptical shape for the power spectrum. For this reason, we fitted the power spectrum by means of a bidimensional circular Gaussian. The same happened in the case of 324 Bamberga, but in this case the resulting discrepancy with the IRAS diameter turned out to be significantly smaller.

As for shapes and ellipse orientations, our results turn out to be in an encouraging agreement with published pole solutions. The orientations of the apparent ellipses, in particular, are generally within 10 degrees from the predictions based on one of the pole solutions. In the case of Victoria and Psyche this allows us to discriminate between the two possible pole solutions, although we find for Psyche a much less elongated shape than predicted. In the case of Victoria, we can also confirm that the spin of this object should be prograde (β of the pole in the northern emisphere), since the solution corresponding to the same pole direction, but with an opposite sense of spin (negative β), does not fit adequately the orientation angle Φ. The situation is more uncertain in the case of Thisbe, due to the little differences in axial ratio and orientation corresponding to the two nominal pole solutions. Our measurement of the axial ratio is in good agreement with both possible predictions, whereas the orientation angle turns out to be 15–20 degrees lower than predicted, and then not in a macroscopic disagreement with both available pole solutions. In the case of 135 Hertha, the axial ratio is compatible with practically all the pole solutions, but the position angle tends to be in a better agreement with two solutions, characterized by a small difference in ecliptic longitude, but largely differing in terms of ecliptic latitude. In both cases, our measurements suggest that the sense of rotation should be prograde.

In the cases of the other asteroids of our sample, no comparison is possible, due to the lack of available pole solutions.

We note also that, in addition to the objects listed in Table 2, we have observed the binary asteroid 90 Antiope. This is a well detached system discovered by adaptive optics (Merline et al., 2000). We observed this asteroid without any a priori knowledge of the epoch of best visibility of the system (largest apparent separation of the components) during the first night of our observing run. The V magnitude at the epoch of our observation was fairly close to the instrumental limit. The obtained power spectrum is very noisy. A single-body solution would lead to an average diameter of 178 km, significantly larger than the IRAS radiometric size of 120 km. The general features of the obtained power spectrum might be potentially compatible with a binary solution, but due to the noisy solution we obtain, we cannot conclude that we see really convincing evidence of the presence of fringes, the expected signal from a resolved binary object. On the other hand, we do not know a priori whether the binary companion should have been really visible during our observations (carried out around 00:15 TU of September 30, 2000). It might well be possible that the binary system was not detached during our snapshot, and this might explain qualitatively the peculiar power spectrum and the discrepancy of a single-object solution with the IRAS listed value of size. In principle, even a negative detection could prove to be useful to constrain the orbital properties of the system. But of course, further observations of this object are needed.

4. Discussion and future work

Our speckle observations show that the TNG speckle camera is an effective instrument for the purposes of measuring asteroid sizes and shapes. The results obtained during the first run of observations turned out to substantially confirm the reliability of radiometric size determinations. The situation is forcedly less certain in the case of shapes, due to the lack of any prediction based on previous photometric evidence for several objects in our sample. However, whenever possible, comparisons with photometric-based predictions seem very encouraging. The small sizes of the recorded power spectra of 3 Juno and 324 Bamberga lead to uncertainties that should be solved by means of new observations in the future.

Asteroid observations require certainly a more extensive observational effort in the future, in order to obtain several independent shape measurements for single objects, carrying out observations at different aspect angles. Also the possibility to follow systematically single objects over several hours seems worth taking into account for future observing runs. In this way, one should be able to monitor the steady change in shape and size due to the rotation of the object.

Another obvious field of research is that of binary asteroids. This includes both the possible discovery of new systems and a systematic monitoring of known binaries in order to derive better determinations of the orbits (from which essential physical parameters such as mass, density, and *J*2 can be derived). At present, this can be done only in favorable cases, in which the separation of the components and their brightness difference are suitable. 90 Antiope is an example of an ideal target for future observations, in spite of the negative detection of binarity during our first attempt.

Acknowledgments

We thank the staff of the TNG, and especially R. Dominguez, for their support in the observations. Very useful suggestions and help for the procedures of data reduction by Enrico Marchetti are also kindly acknowledged. The careful reviews by Yu. G. Shkuratov and an anonymous referee helped in greatly improving the paper.

References

Baier, G., Weigelt, G., 1983. Speckle interferometry observations of the asteroids Juno and Amphitrite. Astron. Astrophys. 121, 137–141.

Campo Bagatin, A., Cellino, A., Davis, D.R., Farinella, P., Paolicchi, P., 1994. Wavy size distributions for collisional systems with a small-size cutoff. Planet. Space Sci. 42, 1079–1092.

Cellino, A., Zappalà, V., Di Martino, M., Farinella, P., Paolicchi, P., 1987. Flattening, pole and albedo features of 4 Vesta from photometric data. Icarus 70, 546–565.

Cellino, A., Di Martino, M., Drummond, J., Farinella, P., Paolicchi, P., Zappalà, V., 1989. Vesta's shape, density and albedo features. Astron. Astrophys. 219, 320–321.

Cellino, A., Zappalà, V., Farinella, P., 1991. The size distribution of main-belt asteroids from IRAS data. Mon. Not. R. Astron. Soc. 253, 561–574.

Cellino, A., Gil Hutton, R., Tedesco, E.F., Di Martino, M., Brunini, A., 1999. Polarimetric observations of small asteroids: preliminary results. Icarus 138, 129–140.

Christou, J.C., 1988. Application of Speckle Interferometry techniques: Working with real data, in: Merkle, F. (Ed.), NOAO-ESO Conference on High-Resolution Imaging by Interferometry: Ground-Based Interferometry at Visible and Infrared Wavelengths, ESO Conference and Workshop Proceedings 29, 97–111.

Davis, D.R., Weidenschilling, S.J., Farinella, P., Paolicchi, P., Binzel, R.P., 1989. Asteroid collisional history: effects on sizes and spin, in: Binzel, R.P., Gehrels, T., Shapley-Matthews, M. (Eds.), Asteroids II, Arizona Univ. Press, Tucson, pp. 805–826.

Drummond, J.D., Christou, J.C., 1994. Images of asteroids 1 Ceres, 2 Pallas, and 4 Vesta with adaptive optics at the Starfire Optical Range, in: Ealey, M.A., Merckle, F. (Eds.), SPIE proceedings: Adaptive optics in astronomy. SPIE, Bellingham, WA, pp. 468–471.

Drummond, J.D., Hege, E.K., 1986. Speckle interferometry of asteroids. III-511 Davida and its photometry. Icarus 67, 251–263.

Drummond, J.D., Cocke, W.J., Hege, E.K., Strittmatter, P.A., 1985a. Speckle interferometry of asteroids. I - 433 Eros. Icarus 61, 132–151.

Drummond, J.D., Hege, E.K., Cocke, W.J., Freeman, J.D., Christou, J.C., Binzel, R.P., 1985b. Speckle interferometry of asteroids. II - 532 Herculina. Icarus 61, 232–240.

Drummond, J., Eckart, A., Hege, E.K., 1988. Speckle interferometry of asteroids. IV - Reconstructed images of 4 Vesta. Icarus 73, 1–14.

Drummond, J.D., Fugate, R.Q., Christou, J.C., Hege, E.K., 1998. Full adaptive optics images of asteroids Ceres and Vesta: rotational poles and triaxial ellipsoid dimensions. Icarus 132, 80–99.

Farinella, P., Paolicchi, P., Tedesco, E.F., Zappalà, V., 1981. Triaxial eliquibrium ellipsoids among the asteroids? Icarus 46, 113–123.

Farinella, P., Paolicchi, P., Zappalà, V., 1982. The asteroids as outcomes of catastrophic collisions. Icarus 52, 409–433.

Hestroffer, D., 1998. Photocenter displacement of minor planets: analysis of HIPPARCOS astrometry. Astron. Astrophys. 336, 776–781.

Hestroffer, D., Mignard, F., 1997. Photometry with a periodic grid. I. A new method to derive angular diameters and brightness distribution. Astron. Astrophys. 325, 1253–1258.

Jedicke, R., Metcalfe, T.S., 1998. The orbital and absolute magnitude distributions of main belt asteroids. Icarus 131, 245–260.

Labeyrie, A., 1970. Attainment of diffraction limited resolution in large telescopes by Fourier analysing speckle patterns in star images. Astron. Astrophys. 6, 85–87.

Marchetti, E., Mallucci, S., Ghedina, A., Farinato, J., Baruffolo, A., Munari, U., Ragazzoni, R., 1997.A real-time speckle facility for the Telescopio Nazionale Galileo, in: The Three Galileos: the Man, the Spacecraft, the Telescope. ASSL Series Vol. 220, p.383, Kluwer Academic, Dordrecht/Norwell, MA.

Merline, W.J., Close, L.M., Dumas, C., Chapman, C.R., Roddier, F., Ménard, F., Slater, D.C., Duvert, G., Shelton, C., Morgan, T., 1999. Discovery of a moon orbiting the asteroid 45 Eugenia. Nature 401, 565–568.

Merline, W.J., Close, L.M., Dumas, C., Chapman, C.R., Slater, D.C., 2000. Discovery of companions to asteroids 762 Pulcova and 90 Antiope by direct imaging. Bull. Am. Astron. Soc. 32, 1309.

Ostro, S.J., Hudson, R.S., Benner, L.A.M., Giorgini, J.D., Magri, C., Margot, J.L., Nolan, M.C., 2003. Asteroid radar astronomy, in: Bottke, W.F., Binzel, R.P., Cellino, A., Paolicchi, P., (Eds.), Asteroids III, in press.

Parker, J.W., Stern, S.A., Thomas, P.C., Festou, M.C., Merline, W.J., Young, E.F., Binzel, R.P., Lebofsky, L.A., 2002. Analysis of the first disk-resolved images of Ceres from ultraviolet observations with the Hubble Space Telescope. Astron. J. 123, 549–557.

Ragazzoni, R., Baruffolo, A., Marchetti, E., Ghedina, A., Farinato, J., Niero, T., 2000. Speckle interferometry measurements of the asteroids 10-Hygiea and 15-Eunomia. Astron. Astrophys. 354, 315–320.

Storrs, A., Weiss, B., Zellner, B., Burleson, W., Sichitiu, R., Wells, E., Kowal, C., Tholen, D.F., 1999. Imaging observations of asteroids with Hubble space Telescope. Icarus 137, 260–268.

Tedesco, E.F., Noah, P.V., Noah, M., Price, S.D., 2002. The supplemental IRAS minor planet survey (SIMPS). Astron. J. 123, 1056–1085.

Tsvetkova, V.S., Dudinov, V.N., Novikov, S.B., Pluzhnik, Ye.A., Shkuratov, Yu.G., Vakulik, V.G., Zheleznyak, A.P., 1991. Shape and size of asteroid 4 Vesta: Speckle interferometry and polarimetry. Icarus 92, 342–349.

Zappalà, V., Cellino, A., 1996. Main belt asteroids: present and future inventory, in: Rettig, T.W., Hahn, J.M. (Eds.), Completing the Inventory of the Solar System, ASP Conference Series 107, Astronomical Society of the Pacific, San Francisco, pp. 29–44.

Zappalà, V., Cellino, A., 2001. Formation of asteroid families and delivery of NEO showers from the main belt, in: Marov, M., Rickman, H. (Eds.), Collisional Processes in the Solar System, Kluwer Academic, Dordrecht/Norwell, MA, pp. 303–321.